Separation and Purification Technology 302 (2022) 122097

Contents lists available at ScienceDirect

Separation and Purification Technology

journal homepage: www.elsevier.com/locate/seppur

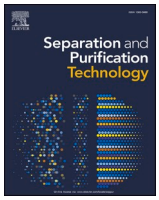

Ultrafiltration-based diafiltration for post-delignification fractionation of lignin from a deep eutectic solvent comprised of lactic acid and choline chloride

Mahsa Gholami [a], Boelo Schuur [a,*], Yagnaseni Roy [a,b,*]

[a] University of Twente, Faculty of Science and Technology, Sustainable Process Technology, PO Box 217, 7500 AE Enschede, the Netherlands
[b] Indian Institute of Science (IISc), Centre for Sustainable Technologies, Bangalore 560012, India

ARTICLE INFO

Keywords:
Ultrafiltration-diafiltration
Deep eutectic solvent (DES)
Lignin recovery
Fouling
Modeling

ABSTRACT

Lignocellulosic biomass is a valuable renewable resource that has the potential to be refined into multiple fractions of valuable biomaterials. Extracting and purifying lignin without compromising cellulose quality is a challenging goal. Deep Eutectic Solvents (DESs) have been reported as suitable delignification solvents, and for process development for cellulose extraction, lignin removal is essential. This work describes an investigation on continuous ultrafiltration (UF)-based diafiltration (DF) for recovering and purifying lignin dissolved in a DES-pulping stream comprising lactic acid and choline chloride following lignocellulose delignification. Experiments have been carried out in a stirred dead-end setup. The results indicate that lignin with a molecular weight of 200 g/mol or higher can be rejected by a polyethersulfone UF membrane with a molecular weight cutoff of 5000, reaching rejection values close to 0.85 for the feed solution with lignin concentration ranging from 4.5 to 30 g/L. It was discovered that membrane fouling and flux decline are DES concentration-dependent. A modeling approach was developed to predict the system size and operating conditions necessary to conduct the diafiltration process on a large scale, for which experimental data on lignin fouling at various feed concentrations and hydrodynamic flow characteristics were used. Based on the modeling results, lignin dissolved in DES-dark liquor (lignin-loaded DES) may well be separated and purified by a continuous UF-DF system.

1. Introduction

To reduce the carbon footprint of production materials such as polymers, replacing fossil-based materials with bio-based materials is a great opportunity that can improve sustainability. Lignocellulosic biomass is the most abundant and sustainable feedstock available in the world. Along with cellulose and hemicellulose, lignin is a major component of lignocellulosic biomass which has a great potential to act as a future source for biofuel and valuable chemicals [1–3]. Valorizing lignin as a production material requires effective isolation method(s). Nowadays, kraft pulping plants are the state-of-the-art in the pulp and paper industry, and commonly accepted as being integrated and energy-efficient plants. In the kraft process, cellulose is isolated from lignocellulosic biomass for use in the pulp and paper industry, which is the primary use of this biomass [4]. The waste stream from this process is called black liquor, which contains highly sulfurized lignin [5,6]. Only 2 % of the lignin finds application, and the rest is burned as low-value fuel [7,8] in the recovery boiler, to recover the solvent from the black liquor. In the last few decades, many studies have focused on either developing a suitable extraction method to recover lignin from the black liquor [9], or developing an alternative energy efficient pulping process, such as organosolv pulping in which sulfur-free lignin may be recovered as a byproduct with beneficial application potential [10]. Recovering lignin allows for complete valorization of the biomass and can be a step toward sustainable production [3].

For an alternative pulping process for biomass treatment, use of deep eutectic solvents (DESs) recently received ample attention, as they have been studied for pretreatment [11–15] and fractionation [16–19] of lignocellulosic biomass and the dissolution of hemicellulose and lignin. DESs are mixtures of two or three components that can form extensive hydrogen bonds with one another, forming a eutectic mixture. The melting points of DES mixtures decrease significantly more (>50 °C) than would be expected for ideal mixtures [20]. Utilizing DESs in the cooking procedure can be considered similar to organosolv, but has advantages over standard acid-based organosolv cooking, as some of the

* Corresponding authors at: Drienerlolaan 5, Meander 221, 7522 KE Enschede, the Netherlands.
E-mail addresses: b.schuur@utwente.nl (B. Schuur), yroy@iisc.ac.in (Y. Roy).

https://doi.org/10.1016/j.seppur.2022.122097
Received 11 July 2022; Received in revised form 6 September 2022; Accepted 7 September 2022
Available online 13 September 2022

Nomenclature

J	Permeate flux (m/s)
R_f	Filtration resistance due to pore-blocking, concentration polarization, and the cake-fouling layer (m^{-1})
R_m	Clean membrane resistance (m^{-1})
R_t	Total filtration resistance (m^{-1})
r)	Rejection (-)
$C_{0,\,DES}$	Initial DES concentration in the feed (g/L)
C_0	Initial lignin concentration in the feed (g/L)
C_p	Lignin concentration in the permeate (g/L)
C_r	Lignin concentration in the retentate (g/L)
X_0	Initial lignin mass fraction in the feed (kg/kg)
X_p	Lignin mass fraction in the permeate (kg/kg)
X_r	Lignin mass fraction in the retentate (kg/kg)
M_p	Total mass flow rate in the permeate (kg/s)
M_r	Total mass flow rate in the retentate (kg/s)
J_s	Lignin mass flux (kg/m^2s)
RR	Recovery ratio (m^3/m^3)
Q_{in}	Inlet feed flow rate (L/h)
Q_p	Permeate flow rate (L/h)
ΔP	Transmembrane pressure (Pa)
ΔP_{loss}	The hydraulic pressure drop along the feed channel, in the feed flow direction (Pa)
f	Friction coefficient (-)
l	Distance along the feed channel (m)
a	Cell surface area (m^2)
x	Coordinate along membrane channel (m)
t	Filtration time ($hours$)
u	Bulk velocity of flow in the feed channel (m/s)
L	Length of the membrane module (m)
W	Width of the membrane module (m)
h	Hydraulic diameter of the feed channel (m; for a rectangular channel ($H \ll W$), h = 2H
H	Height of the feed channel (m)

Greek symbols:

ϑ	Kinematic viscosity (m/s)
μ_p	Permeate viscosity ($Pa.s$)
ρ_p	Permeate density (kg/m^3)
ρ	Density of the feed (kg/m^3)

Dimensionless parameters:

Re	Reynolds number ($Re = \frac{uh}{\vartheta}$)

DES constituents, such as halogen anions, can have catalytic behavior [21,22].

The sustainable fractionation of lignin from the stream after delignification process requires cost-effective, energy efficient, and environmentally-friendly separation methods. Cold water precipitation and liquid–liquid extraction using an organic solvent have been studied as promising methods for extraction of lignin dissolved in the DES-based black liquor after delignification [23]. However, the complexity of the stream is such that a single separation method is not sufficient to completely fractionate the DES-based black liquor and isolate all fractions including lignin [24]. Recent studies by Smink et al. showed that lignin dissolved in DES comprised of lactic acid and choline chloride after DES-delignification can be extracted into 2-methyltetrahydrofuran (2-MTHF), using liquid–liquid extraction (LLX) [25]. However, to limit the leaching of lactic acid, the composition of the DES should be chosen with a relatively large amount of choline chloride [26]. To maximize the flexibility of DES-based delignification, it is wise to investigate on a variety of downstream separation techniques that may complement each other. Therefore, going beyond the water precipitation and LLX-based approaches, in this work membrane-based separations have been explored as potential separation technique in the toolbox for lignin removal [27].

Ultrafiltration (UF) is likely to be applicable to concentrate lignin from DES-based dark liquors. [28–31]. However the retentate in single stage membrane operations will always contain DES therefore further dilution with a diluting solvent is required to lower the DES concentration in the lignin-rich retentate in order to obtain as pure lignin as possible. Applying UF with a diluting solvent basically resembles a diafiltration method, is called ultrafiltration-based diafiltration (UF-DF) [32,33]. The schematic shown in Fig. 1 involves an ideal continuous DF without any pressure loss, although this method can be implemented in a batch mode as well [34].

The continuous diafiltration has been implemented for separation and purification of byproducts from waste stream in food industries such as in the production of coffee [35] or preparation of milk protein concentrates [36]. This process consists of three stages: 1- a pre-concentration using UF membranes which reduces the volume of the feed solution and hence increases the concentration of the higher molecular weight species in the membrane retentate stream; 2- dilution of the retentate stream from step 1, using a solvent to dilute the lower molecular weight species as much as possible while simultaneously permeating this diluted feed through the membrane, thereby removing the lower molecular weight species from the higher weight species; 3 - final concentration step by permeating the solvent through the

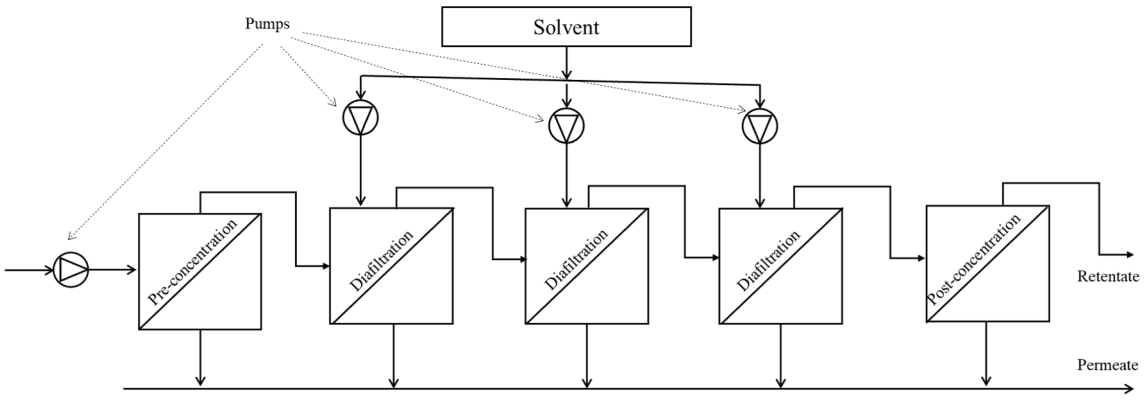

Fig. 1. Principle of continuous ultrafiltration-based diafiltration (UF-DF).

membrane and thereby increasing the concentration of the larger molecules [32].

Previous works on UF-DF for lignin isolation have shown great potential for treatment of black liquor after biomass delignification [37–39]. For example, Servaes et al. focused on lignin recovery from the kraft process, and demonstrated that UF-DF process can be a promising technique for purifying and concentrating lignin dissolved in black liquor following delignification of wood chips in an alkaline oxidation process with a purity of 94 % in the high molecular weight fractions [27]. This is a purity approximately 10 % higher than the purity reported by Tanistra and Bodzek [40]. They concentrated and purified kraft lignin using both continuous and batch diafiltration. An observation from the existing literature on UF-DF as discussed above is that none of these studies discussed the influence of membrane fouling as the filtration process proceeds. Since membrane fouling is known to be one of the major challenges in membrane [41,42], this aspect deserves attention for the prediction of long-term operation of the system, and will dictate practical considerations such as changing flux permeation rate with time, and hence the required system size to continue the process over a reasonably long operating period.

Many mathematical models have been proposed to characterize the flow decrease and fouling in membrane filtration, either using or improving Hermia's equation [43], which describes the fouling mechanism in the dead-end filtration process [44], or based on a resistance-in-series model, which describes the flow reduction as the fouling resistance increases over time [41,45,46]. Since modeling of fouling in DF systems with lignin feed is missing in the literature, and it is key to describe longer term flux behavior, we aim to describe fouling in UF-DF of lignin from DES in the current work. To help process development to minimize fouling, the effects of membrane fouling will be predicted using a numerical simulation-based approach, for the development of which, experimental results will be used as input to yield the most accurate modeling results possible [47].

The UF-DF process studied in this work was applied in a solvent-diluted stream that in a full process is obtained from washing out remaining lignin from the obtained fibers by delignification. Thus, the lignin dissolved in the DES comprised of lactic acid and choline chloride obtained after delignification was diluted with a 70:30 (v:v) acetone–-water mixture, suitable for this due to the high solubility of lignin in this mixture [48]. Using experimental results on lignin fouling at various feed concentrations and hydrodynamic flow conditions, a modeling approach was developed to predict the system size, and make recommendations on operating conditions in order to implement the UF-DF process over a reasonable long period of time.

2. Experimental technique and equipment

2.1. Chemicals used

The solvent used in this study was prepared using MilliQ water and technical grade acetone from Boomlab in The Netherlands. To prepare the DES, 90 wt% lactic acid in aqueous solution from VWR Chemicals and choline chloride (98 wt%) from Sigma Aldrich were combined in a weight ratio of 10:1 (dry lactic acid to choline chloride). Alkali low sulfonate-content kraft lignin from Sigma Aldrich which is similar with extracted lignin from DES-pulping in weight average molecular weight (Mw), number of average molecular weight (Mn) and polydispersity index (PDI) (Supplementary information S1) was combined with DES and a mixture of acetone–water (70:30 vol ratio) to produce lignin feed solutions ranging from 4.5 to 30 g/L, considering the lignin solubility in acetone–water (70:30 v:v) is around 30 g/L [48].

2.2. Membrane used

Experiments were done using an ultrafiltration flat sheet membrane (GR90PP) from Alfa Laval with molecular weight cutoff (MWCO) of 5000 Da [49]. The membrane is polyethersulphone polymer based with polypropylene (PP) support material. Preservatives were removed from the membrane samples by soaking them overnight in MilliQ water. To remove any residual preservatives, the membranes were flushed for 30 min at 10 barg with MilliQ water.

2.3. Experimental setup

A pressurized and mechanically stirred dead-end filtration setup with capacity of 1 L was used, as displayed in supplementary information S2. The filtration cell has a diameter of 75 mm and an effective membrane area of 44.2 cm^2. The mechanical stirrer facilitates agitation of the feed solution over the membrane surface, simulating crossflow flow conditions to bring it closer to industrial practice. A pressure gauge was used to monitor the pressure in the filtration cell, and a pressure regulator was used to control it. Nitrogen gas was used for pressurization. A Kern DS8K0.05 weighing scale with an accuracy of 0.05 g and a capacity of 3 kg that is attached to a computer to read data is used to record the weight of permeate over time.

2.4. Chemical analysis

Chemical analysis of retentate, permeate, and feed samples was performed using an Agilent 1260 Infinity Gel Permeation Chromatography (GPC). The GPC machine was equipped with a UV detector running at 254 nm, a refractive index detector, and 3 GPC PLgel 3 m MIXED-E column series. The column was operated at 40 °C and a 95:5 (v:v) tetrahydrofuran and water mixture as mobile phase. The mobile phase flowrate was kept at 1 ml/min. Molecular weight distributions were calibrated using polystyrene solutions having molecular weights ranging from 162 to 27,810 g/mol.

2.5. Viscosity and density measurement methods

An Ubbelohde viscometer was used to measure viscosities at room temperature of 22 °C (±2 °C). The viscometer has an extended uncertainty of 0.17 % and was calibrated by Paragon Scientific ltd. The viscosity data is based on the primary standard of pure water at 20° C (ITS-90), having a 0.17 % uncertainty and adopted by NIST, ASTM, ISO, and IP. All measurements were done in duplo, with an uncertainty of $\pm 3 \times 10^{-3}$ mPa s.

To determine the densities of samples with different lignin and DES concentration, weight of known volume of solutions were measured using a 10 ml volumetric flask and Mettler AT200 balance.

2.6. Experimental procedure

All experiments were carried out at room temperature of 22 °C (±2 °C). For each experiment a new membrane sample was used which had been cleaned of preservatives by the method stated in Section 2.2. For all experiments, prior to contact with the feed solution, the membranes were flushed for 30 min with the solvent used to make lignin feed solutions i.e., acetone–water (70:30 v:v) at 10 barg to evaluate the clean membrane resistance, taking into account that membrane swelling will reach pseudo-equilibrium state in less than 30 min. All experiments were run at a pressure of 10 barg for a time duration sufficient to filter at least 100 ml of feed solution. Each experiment is repeated three times with different membrane samples but the same feed solutions. To check the durability of membrane against solvent (acetone–water) a piece of membrane was immersed in acetone–water (70:30 v:v) for 1 month and then permeation flux of the lignin solution was measured. Results have been reported in the supplementary information S3.

The permeate flux was measured over time using the weighing scale and density of solution as described in Eq. (1):

$$J = \frac{1}{A}\frac{dM}{\rho_p dt} = \frac{1}{A}\frac{dV}{dt} \quad (1)$$

where A is active membrane area in m^2, M and V are permeated mass (kg) and permeated volume (m^3), respectively. The term ρ_p is the density of permeated solution in (kg/m^3), and t is the filtration time in seconds.

2.7. Mathematical formulation for data analysis

The flux through the membrane can be calculated using Darcy's law:

$$J = \frac{\Delta P}{\mu_p R_t} \quad (2)$$

where ΔP is transmembrane pressure (Pa) and the viscosity of permeate is denoted as $\mu_p(Pa.s)$.

In Darcy's equation (Eq. (2)), R_t is total resistance (m^{-1}), i.e. the total resistance to permeation due to the intrinsic membrane resistance, pore-blocking, fouling cake layer formation, and concentration polarization (CP) [50,51]. The value of R_t will be calculated using flux data and the viscosity of the permeate for each trial:

$$R_t = \frac{\Delta P}{\mu_p J} = R_m + R_f \quad (3)$$

where R_m is the clean membrane resistance and can be calculated using the solvent flux and viscosity, R_f is the resistance to filtration caused by pore blockage, cake formation, and concentration polarization, collectively referred to as filtration resistance.

The lignin rejection is defined using Eq. (4):

$$r = 1 - \frac{C_p}{C_r} \quad (4)$$

C_p and C_r are the lignin concentrations of solution (g/L), in the permeate and retentate sides respectively.

3. Results and discussion

To develop a design approach for a membrane system to recover lignin from DES by UF-DF, an experimental study to investigate the influence of diafiltration operating conditions on lignin rejection, flux decline, and fouling resistance during filtration, has been conducted. Results from this set of investigations are discussed here and used as inputs to the model.

3.1. Experimental results

3.1.1. Effects of stirrer velocity and feed lignin concentration on lignin rejection and filtration resistance

The effect of the lignin concentration on the lignin rejection and filtration resistance of the feed solution was studied to gain understanding on how fluctuating concentrations of lignin during a continuous diafiltration process as shown in Fig. 2, impact on the performance. Therefore, experimental investigation of the conducted. As the feed flow rate varies across the diafiltration system, mass transfer characteristics in the modules will be altered accordingly. To investigate the effect of altering feed flow rate on lignin rejection and cake layer resistance due to lignin fouling, the speed of the mechanical stirrer was adjusted to a high stirrer velocity (1258 rpm), low stirrer velocity (518 rpm), and to the no stirring condition. At the end of the filtration process, the filtration resistance and lignin rejection were calculated using Eqs. (3) and (4). As indicated in section 2.6, pure solvent flux (acetone–water (70:30 v:v)) at the given pressure was employed in Eq. (3), to calculate the clean membrane resistance ($R_t = R_m$). The calculated R_m for all trials was 8.5 $\times 10^{13}$ ($\pm 5\%$) m^{-1} (the accuracy being the relative standard deviation of thirty clean acetone-water flux measurements).

The ratio of peak areas of GPC chromatograms of the retentate and permeate samples, were used to compute the ratio of lignin concentrations of solution in permeate and retentate side presuming lignin will be exhibited by molecular weight of 200 g/mol and higher [16,24]. In the supplementary information S4, GPC chromatograms of the retentate and permeate from experiments with 15 g/L feed lignin solution are provided. As shown in Figure S4 (a), there is no rejection for molecules with an apparent molar weight below 200 g/mol which includes the DES components, i.e. lactic acid (90.08 g/mol) and choline chloride (139.62 g/mol).

Fig. 3 (a) and (b) show that having a well-mixed feed solution during filtration significantly reduces filtration resistance, as the filtration resistances of the stirred experiments were significantly lower than the resistance in the experiment without stirring. There was no significant difference in filtration resistance between the 1258 and 518 rpm stirring rates. The higher the lignin concentration, the higher the filtration resistance and, as a result, the higher the lignin rejection due to a thicker fouling layer on the membrane's surface that prevents lignin from passing through.

The filtration resistances for both stirrer velocities being significantly lower when compared to the no stirring condition, is explained by the reduced CP layer that prevents lignin molecules from reaching and accumulating on the membrane's surface [42]. When there is no agitation during filtering, however, lignin rejections are smaller. Because the molecules' back-diffusion to the bulk is not enhanced by the agitation, they can more readily reach the surface of the membrane and transport through.

3.1.2. Effects of stirrer velocity and feed lignin concentration on flux decline

To study the effect of stirrer velocity on flux decline behavior, the flux decline over time was plotted for trials with a constant lignin concentration of 15 g/L and DES concentration of 229 g/L and varied stirrer speeds of 1258 rpm, 518 rpm, and no stirring. As shown in Fig. 4 (a), non-stirred filtration results in a rapid reduction in flux to a much lower flux than with stirred filtration, while the fluxes in both stirred experiments show similar behavior, exhibiting a very gradual decline after the initial strong reduction in flux. It should be noted that for both non-stirred and stirred filtration, the filtration flux using the lignin feed was significantly lower than the flux of pure solvent in the experiments done for calculation of R_m. The reduced flux is due to the pore blocking or/and establishment of cake filtration and of a CP layer [52].

Fig. 4 (b) shows the permeation flux over time for a set of experiments with varying lignin concentrations with a stirrer speed of 1258 rpm. The flux does not alter when the feed lignin concentration is increased from 4.5 to 30 g/L, and at each lignin concentration, the flux decreases rapidly at first owing to membrane pore blocking and development of the CP layer [52,53], after which a slow gradual decline in flux due to the establishment of cake filtration is observed which is very similar for all lignin concentrations. The maximum relative uncertainty in all measurements was within the range of ±8–10 % (L/m^2 h).

3.1.3. Effects of initial DES concentration on flux decline and filtration resistance

Since the DES concentration decreases along the system in the continuous UF-DF process, as solvent is added, the impact of DES concentration on flux pattern and filtration resistance should be experimentally evaluated. The lower the DES concentration in the feed solution, the lower the viscosity and density (values shown in supplementary information S5).[1]

To study the effect of DES concentration on flux reduction and

[1] Results in Supplementary information S5 show that the viscosity and density of all feed concentrations are the same as the viscosity and density of the permeate solution, and that they are not dependent on lignin concentration.

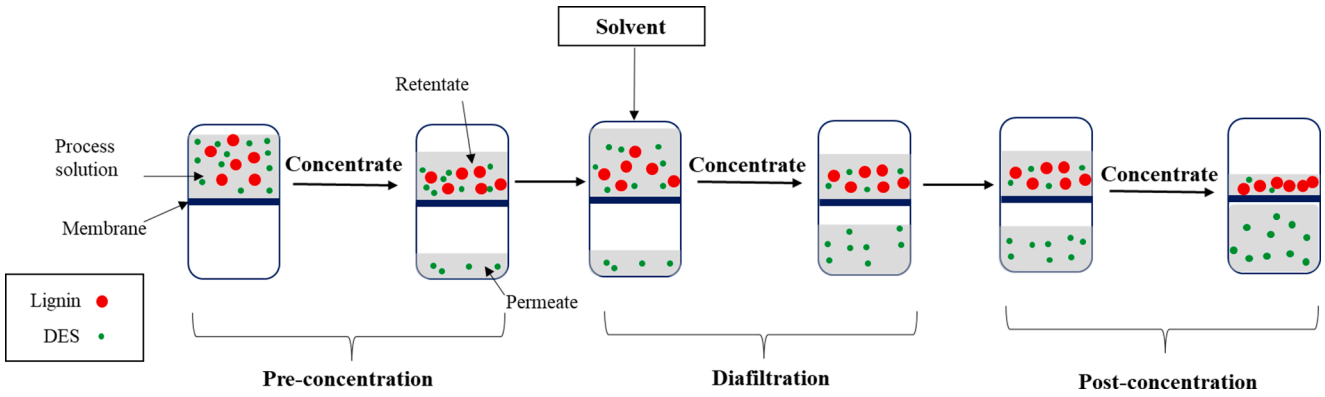

Fig. 2. Concept of separation of lignin from DES using ultrafiltration-based diafiltration process (UF-DF).

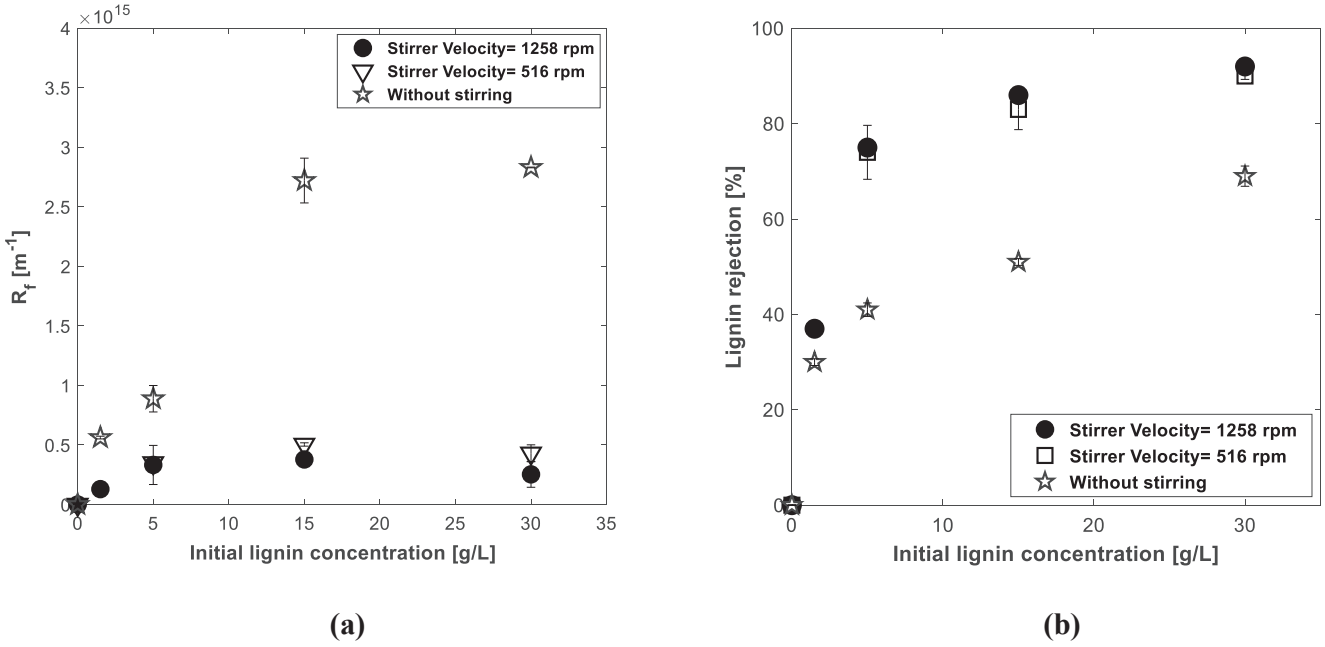

Fig. 3. Effects of stirrer velocity and initial lignin concentration on lignin rejection and filtration resistance: (a) filtration resistance for filtration trials under different stirrer velocities (1258 rpm, 516 rpm, and no stirring i.e. 0 rpm) versus the lignin concentration in the feed at 10 barg, (b) lignin rejection for filtration trials under different stirrer velocities versus the lignin concentration in the feed at 10 barg.

filtration resistance, the lignin content was held constant at 15 g/L while the DES concentration was varied from 229 g/L to 46 g/L. These DES concentrations correspond to the initial DES concentration entering the UF-DF process, and DES concentration considering adding solvent with dilution factor of 5 in single-stage diafiltration. For both feed solutions, the stirrer velocity was set at 1258 rpm. Fig. 5 (a) depicts the reduction of flux for feeds with 46 g/L DES and 229 g/L DES. As can be observed, at the average flux increases as the amount of DES in the feed is reduced due to lower viscosity and density of the permeate solution. Moreover, feed with higher DES concentration shows a sharper initial flux decline caused by higher initial pore blocking or greater CP layer. Considering that there is no rejection for smaller components including DES in either filtration condition, it is possible that increased DES concentration (higher lactic acid) causes de-swelling of the membrane polymer, resulting in smaller pores in the membrane and consequently more pore blocking and a sharper flux decline.

Fig. 5 (b) shows changing in filtration resistance over time for both feed with 229 g/L DES and 46 g/L DES concentration. A linear regression of filtration resistance over time can be applied in both circumstances following a dramatic increase in filtration resistance due to initial pore blocking or/and development of CP layer. This indicates that the fouling layer is gradually accumulating following the initial significant flux drop. The rate of increase in filtration resistance caused by fouling development, is generally constant over time and strongly dependent on DES concentration. These correlations may be utilized to predict the development of fouling layers in numerical simulations for large-scale UF-DF.

3.2. Model development

In this section a modeling approach to design an industrial scale UF-DF system is developed. Numerical modeling was utilized to simulate the establishment of a fouling layer following the initial sharp decrease in flux in an industrial scale of UF-DF system in order to determine the required membrane area for such a system.

3.2.1. Membrane channel

A flat-sheet membrane configuration as displayed in Fig. 6, was considered for modeling [54,55]. The model was numerically solved using MATLAB (version R2020b) and the algorithm is shown in

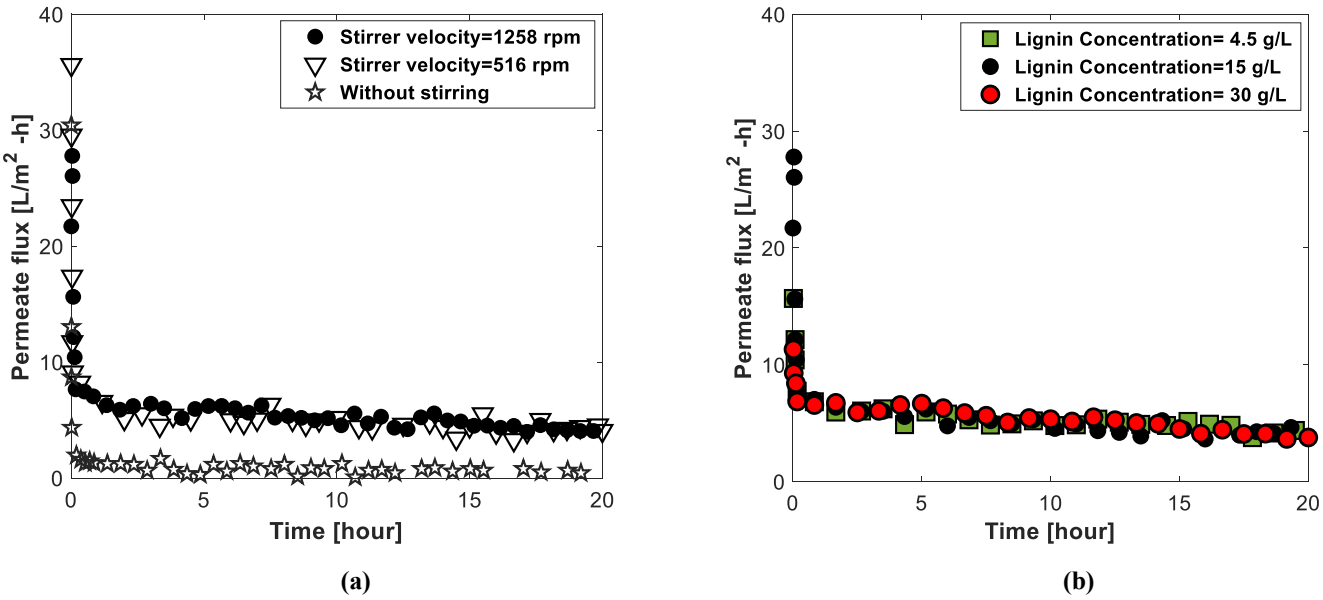

Fig. 4. Effects of stirrer velocity and initial lignin concentration on flux decline: (a) flux decline for filtration trials under different stirrer velocities at 10 barg with same DES concentration = 229 g/L, (b) flux decline for filtration trials with different lignin concentration in feed (DES concentration = 229 g/L, stirrer velocity 1258 rpm, 10 barg).

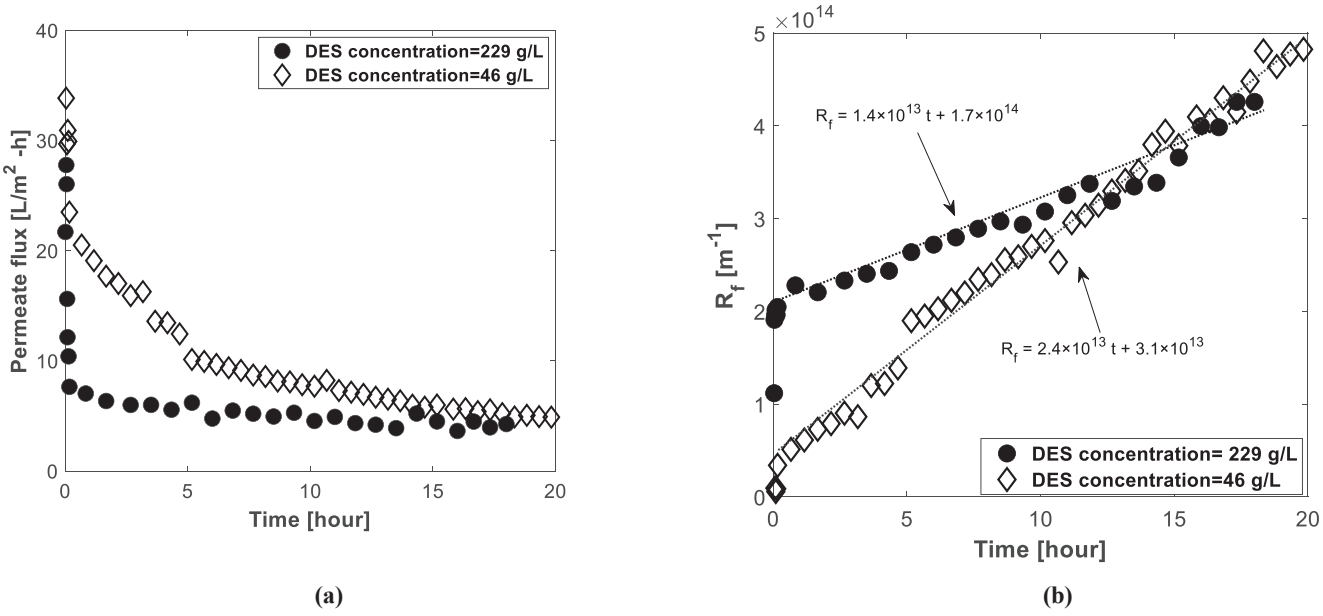

Fig. 5. Effects of initial DES concentration on flux decline and filtration resistance: (a) Flux decline of feeds with different DES concentration (lignin concentration = 15 g/L, stirrer velocity: 1258 rpm), (b) change in fouling resistance over time for feed with different DES concentration.

supplementary information S6. The membrane channel was split into at least 400 cells for all of the simulations in this study.

Table 1 shows the values of the simulation's parameters. The amount of additional solvent required in each diafiltration stage is four times the volume of feed solution entering that stage, which can later be recovered through other separation techniques, such as evaporation or membrane separation. The clean membrane resistance (R_m) and lignin rejection (r) has been considered 8.5×10^{13} m^{-1} and 0.85, respectively, based on the experimental results presented in section 3.1.1.

3.2.2. Model formulation

Based on the experimental results, described in section 3.1.3, Fig. 5 (b), R_f can be expressed as function of filtration time via Eq. (5):

$$R_t - R_m = R_f = At + B \tag{5}$$

where A and B are adjustable parameters and were fixed based on the changes in the DES concentration, from pre-concentration to the diafiltration steps, at any location in the x-direction and in the fixed time. As long as the fouling layer has not achieved its steady-state thickness, this equation can be applied [28].

Using Eq. (5) and Darcy's law (Eq. (2)), the permeation flux ($m^3/m^2.s$) can be calculated at given time (t) and location x(i):

$$J^i = \frac{\Delta P^i}{\mu_p R_t^i} = \frac{\Delta P^i}{\mu_p (R_f + R_m)^i} \tag{6}$$

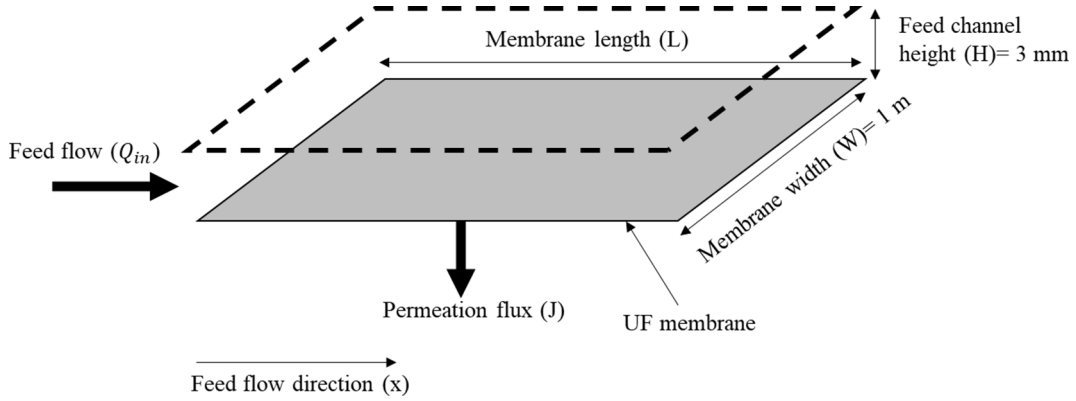

Fig. 6. Schematic description of membrane feed channel.

Table 1
Parameters for modeling a full-scale continuous UF-DF process.

Channel height, H (m)	3×10^{-3}
Membrane width, W (m)	1
Applied pressure, ΔP_0 (Pa)	10^6
Initial lignin concentration, $C_{0,\,lignin}$ (g/L)	4.5
Initial DES concentration, $C_{0,\,DES}$ (g/L)	229
Initial feed flow rate, Q_{in} (L/h)	100
Lignin rejection (r)	0.85
Number of cells along the membrane channel	400
Clean membrane resistance, R_m (m^{-1})	8.5×10^{13}
Number of diafiltration stages	3
Ratio of volume of added solvent to volume of initial feed for each diafiltration step	4

Equation (7) is used to calculate the transmembrane pressure along the membrane system:

$$\Delta P^i = \Delta P^{i-1} - \Delta P_{loss} \tag{7}$$

The correlation of friction coefficient in the feed channel from [56], has been used to calculate the hydraulic pressure drop over the length of the membrane at given location x(i), along the feed flow direction (Eq. (8)):

$$f = \frac{6.23}{Re^{0.3}} \tag{8}$$

$$\Delta P_{loss} = \frac{f}{2}\frac{l}{h}\rho u^2 \tag{9}$$

The pressure-drop along the feed channel, in the feed flow direction is calculated by Eq. (9) [57]. In this equation, u is the bulk velocity of flow at that location, h is the hydraulic diameter of the feed channel (m), l is the length along the membrane channel in the feed flow direction at given location x(i) (m) and ρ is the density of feed flow. The permeate flow rate is less than the feed flow rate. Consequently, the permeate Reynolds number is low, and the hydraulic pressure loss is negligible. As a result, for the permeate side atmospheric pressure is assumed [58,59].

The lignin mass fraction in permeate side is expressed using lignin mass fraction in retentate side and rejection value:

$$r = 1 - \frac{C_p}{C_r} = 1 - \frac{\rho_p X_p}{\rho_r X_r} = 1 - \frac{X_p}{X_r} \tag{10}$$

$$X_p = X_r(1 - r) \tag{11}$$

X_r and X_p are the mass fractions of lignin in the retentate side and permeate side. ρ_p and ρ_r are the densities of solution in permeate and retentate side, respectively. The experimental results show that the density of lignin in fixed amount of DES and acetone–water is independent of lignin concentration (Supplementary information S5). Therefore, ρ_p and ρ_r can be considered equal. For all calculations, the lignin rejection was set to 0.85. Fixing the rejection eases the calculations at any position in the x-direction, and from Fig. 3, it follows that although there is a small dependency of the lignin rejection on the lignin concentration for the range of 4.5 g/L $< 30C_{lignin} <$ g/L, with the average of 0.85.

M_r and M_p refer to total mass flow rate in retentate and permeate side (kg/s). As a result, in a given time step during the modeling along the membrane cell at location x(i):

$$M_r^i = M_r^{i-1} - a\rho J^{i-1} \tag{12}$$

$$M_p^i = M_p^{i-1} + a\rho J^{i-1} \tag{13}$$

$$X_r^i = \frac{X_r^{i-1}M_r^{i-1} - J_s^{i-1}a}{M_r^i} \tag{14}$$

$$X_p^i = X_r^i(1 - r) \tag{15}$$

where a is cell surface area and is measured by dividing the channel membrane area by the considered number of cells and J_s is the lignin mass flux in each cell as follows:

$$J_s^i = \rho J^i X_p^i \tag{16}$$

The recovery ratio for each membrane system is defined as the ratio of total permeate flow rate (Q_p) leaving the module at given time, divided by feed flow rate (Q_{in}) entering the module. Since the densities of permeate and feed solutions have been considered equal, recovery ratio at given time step is expressed by total mass of permeate divided by initial mass of feed as follow:

$$RR = \frac{Q_p}{Q_{in}} = \frac{M_p^i(i = N)}{M_r^i(i = 0)} \tag{17}$$

The prediction model for a full-scale continuous UF-DF filtration system is formed by Eqs. (5)–(17).

3.2.3. Modeling results

The lignin concentration profile at the beginning of fouling formation, after rapid flux decline $(t = 0)$ along the membrane system is depicted in Fig. 7 (a). As can be noticed, considering a width of 1 m for all membrane systems, a pre-concentration step with a membrane area of 13 m^2 followed by three steps of diafiltration with areas of less than 2 m^2, is required to concentrate the lignin stream to 30 g/L which has been considered as maximum solubility of lignin in acetone–water (70:30 v:v). It should be underlined that in this condition, pore blocking resistance, CP layer resistance, and clean membrane resistance predominate, as the fouling layer has not yet developed. As a result, the appropriate

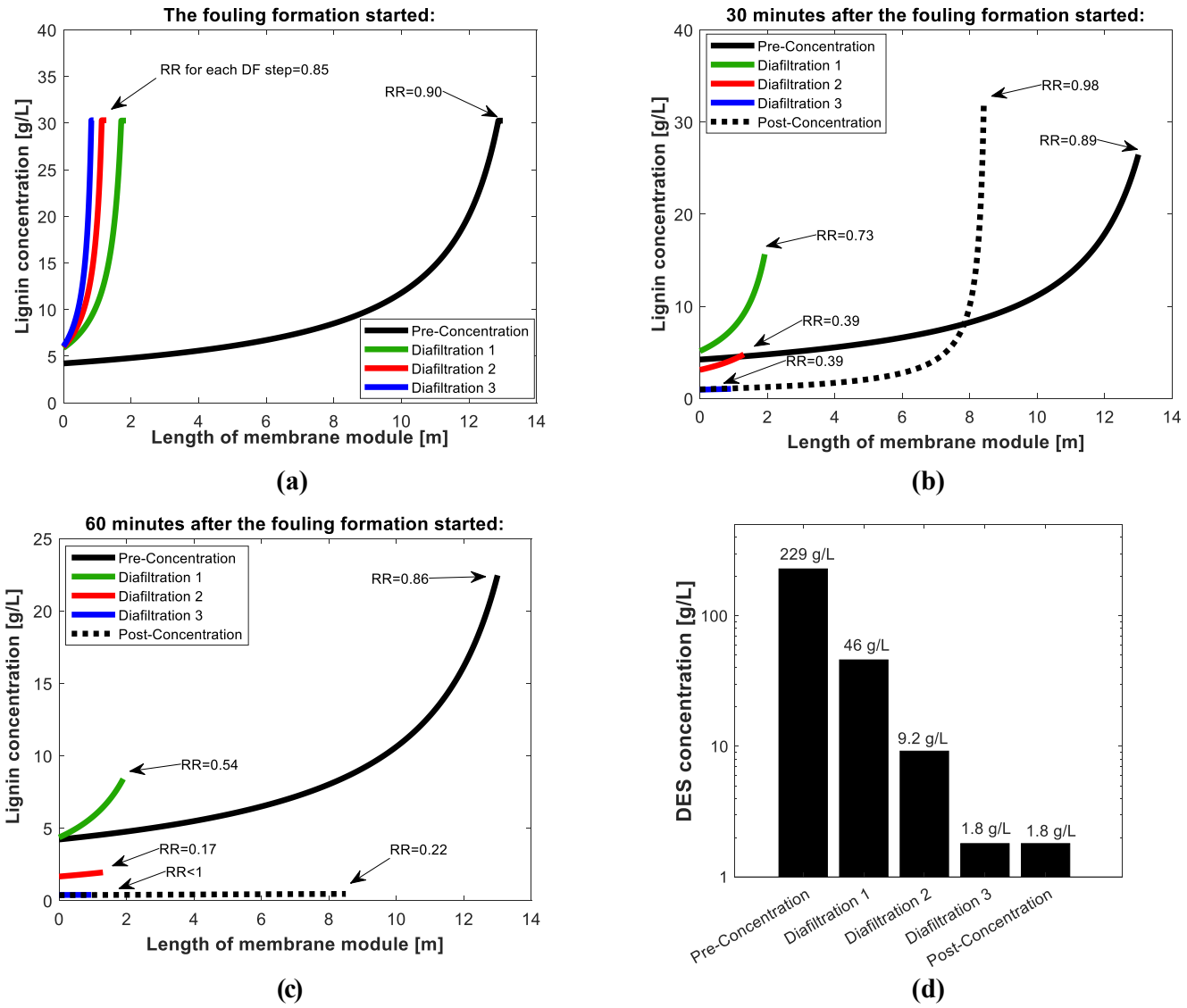

Fig. 7. Lignin concentration along the membrane channel for: (a): t = 0 (the initiation of fouling formation after the sharp flux decline), (b): t = 30 min (30 min after the fouling formation initiated), and (c): t = 60 min (60 min after the fouling formation initiated.) in modeled UF-DF system. RR is the recovery ratio in each step calculated using Eq (17), (d): DES concentration in the retentate side of each step of modeled UF-DF system.

recovery ratio is attained.

The lignin concentration profile 30 min after the gradual flux decline zone initiated, for the same system size, is shown in Fig. 7 (b). Despite the fact that the fouling layer grows throughout this time period, the recovery ratio in pre-concentration and first diafiltration remains more than 0.7, allowing the lignin concentration to be increased to approximately 15 g/L and the DES concentration to be decreased to 46 g/L, which is approximately 5 times less than the initial DES concentration. However, the increasing volume of feed entering the diafiltration steps due to the addition of solvent, and the growth of the fouling layer reduces the recovery ratio for the second and third diafiltration steps. As a result, the volume of lignin solution entering the post-concentration step grows after one hour as well, therefore the membrane area for post-concentration module is insufficient to achieve maximum lignin concentration after one hour (Fig. 7 (c)). Consequently, backwashing is necessary to remove the fouling layer and keep the membrane system working for an extended period of time.

The DES content in this modeled membrane system will be lowered from 229 g/L to 1.8 g/L by injecting acetone–water as the solvent in three steps of diafiltration, as indicated in Fig. 7 (d). It should be highlighted that since there is no rejection of DES components by this UF membrane, the concentration of DES remains constant over the length of each step of this UF-DF system.

Fig. 8 (a) depicts flux along the membrane system consisting of one pre-concentration step and three diafiltration steps with the above-mentioned size at the start of fouling formation (t = 0) where the clean membrane resistance, membrane pore blocking and CP layer are dominant. Due to the high DES content of the feed, flux is considerably lower in the pre-concentration step compared to diafiltration steps. Adding solvent during the diafiltration steps reduces the DES content of the feed stream, decreasing the filtration resistance and resulting in a higher flux. It is important to note that permeate flux decreases slightly in each phase of the membrane system along the membrane due to changes in lignin concentration and pressure drop; however, because the difference in flux from pre-concentration to diafiltrations and post-concentration is so large, it is not visible in this plot.

Fig. 8 (b), depicts the profile of permeate flux in various time steps over the length of the membrane module for the pre-concentration stage. As can be seen, the flux will decrease over time as the fouling layer grows on the membrane's surface, hence increasing flux resistance. However, as demonstrated by experimental results (Section 3.1.2 and 3.1.3), the permeate flux steadily decreases following a significant

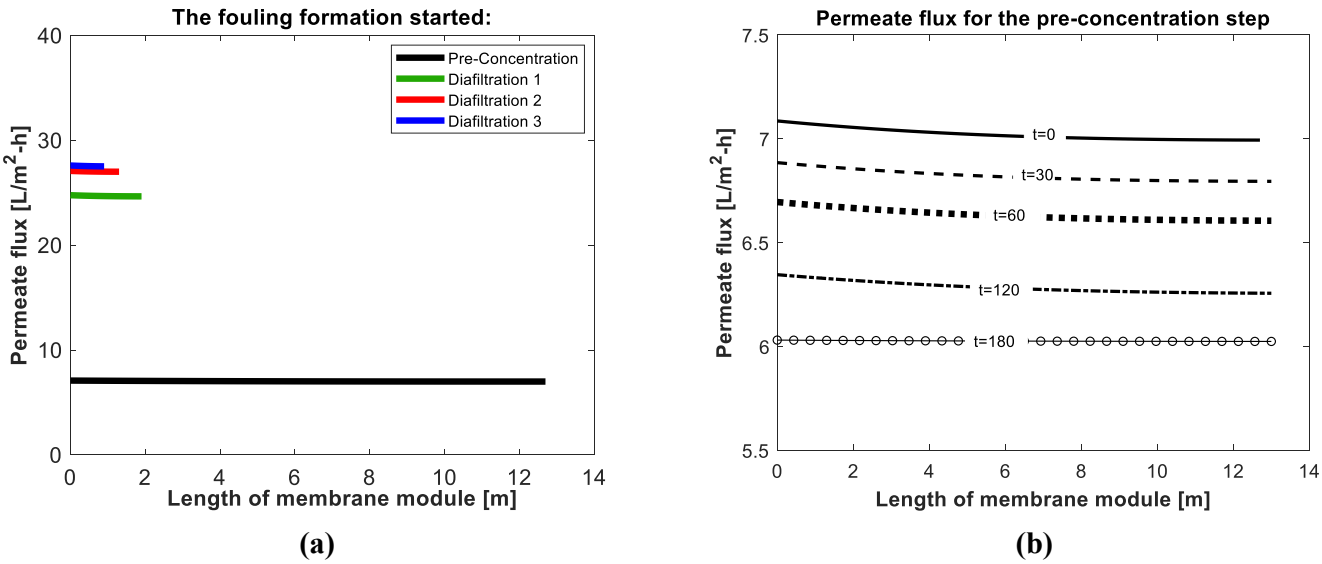

Fig. 8. (a) Permeate flux over the length of the membrane module at t = 0 (the fouling formation initiated) for the UF-DF system, (b) permeate flux over the length of the membrane module with increasing operational time for the pre-concentration step.

decrease at the beginning of filtration. This is likewise true for all diafiltration steps and post-concentration.

Based on modeling results, using a continuous UF-DF system with an initial flow rate of 100 L/h feed solution containing 4.5 g/L lignin and 229 g/L DES and continuously adding solvent in three steps, the final retentate would be highly lignin concentrated with low DES content. With this composition, isolating the lignin from this stream can be done by evaporation of (a part of) the acetone from this retentate stream. Reducing the acetone content and increasing the lignin content will cause lignin to precipitate. Only marginal amounts of water will likely need to be evaporated, as lignin solubility in water is very low, and upon removal of the acetone, precipitation will be induced. By thus avoiding the evaporation of large amounts of water, one can lower the overall cost and energy needs of the operation. Future studies should focus on a detailed estimation of the required energy for recovering lignin from the retentate stream. Recovery of DES from the permeate stream should be further studied. It is worth noting that the employed Alfa laval UF membrane is designed for the treatment of water-based streams, and utilizing a solvent-resistant membrane for the current application may improve the permeation flux while improving the lignin rejection, and therefore minimize the required size of the membrane system.

4. Conclusions

A continuous UF-DF process was investigated to recover and purify lignin dissolved in a DES made of lactic acid and choline chloride after delignification of lignocellulose biomass. A numerical modeling approach was developed based on experimental data on lignin fouling at various feed concentrations and hydrodynamic flow parameters in order to properly assess the required system size and operating conditions to conduct the diafiltration process. The following are the key findings of this study:

1- The commercial Alfa laval polyethersulphone polymer-based membrane with MWCO 5000 Da (GR90PP) was investigated for lignin rejection in an aqueous acetone solvent using a stirred-cell dead-end setup, and this membrane showed high rejection for all feed concentrations of lignin (average of 0.85 for all operation conditions (Fig. 3 (b))).
2- The flux is higher for stirred filtration than for filtration with no stirring; consequently, filtration resistance is lower for stirred filtration than that with no-stirring due to the thinner concentration polarization layer and, more notably, because stirring prevents lignin particles from reaching and accumulating on the membrane's surface which would lead to fouling.
3- The filtering resistance changes when the DES-content of the feed solution changes. The more the DES concentration of the feed, the greater the pore blockage caused by lignin. This is because the higher DES concentrations most likely cause de-swelling of the membrane polymer, resulting in smaller holes in the membrane and, as a result, increased pore blockage and a steeper flux drop.
4- The modeling findings demonstrated that a continuous UF-DF system can separate and purify lignin dissolved in DES-dark liquor from the remaining solutes by utilizing acetone–water as a solvent. Because of the higher filtration resistance and accordingly lower flux for the feed with high DES content, the needed size of such a system at the pre-concentration stage is found to be considerable. However, the size of the system for the diafiltration stages and post-concentration is predicted to be smaller, thereby allowing the total system size to be reasonable.
5- Calculation of the required energy to recover lignin from the retentate stream, and that to recycle the solvent from the permeate stream should be made. The rejection of the lignin under the industrially-favorable crossflow conditions can be more accurately determined using a lab-scale crossflow setup in later work.

CRediT authorship contribution statement

Mahsa Gholami: Investigation, Methodology, Writing – original draft. **Boelo Schuur:** Supervision, Project administration, Funding acquisition, Writing – review & editing, Methodology. **Yagnaseni Roy:** Conceptualization, Supervision, Writing – review & editing, Methodology.

Declaration of Competing Interest

The authors declare that they have no known competing financial interests or personal relationships that could have appeared to influence the work reported in this paper.

Data availability

Data will be made available on request.

Acknowledgements

This project is called PRIDES and is co-funded by the Institute for Sustainable Process Technology (ISPT) and TKI E&I with the supplementary grant 'TKI-Toeslag' for Topconsortia for Knowledge and Innovation (TKI's) of the Ministry of Economic Affairs and Climate Policy. The authors would like to thank all members of the ISPT Consortium for their contribution. The consortium consists of the following organizations: BASF, CTP, CTST, Mayr-Melnhof, Mid Sweden University, Mondi, Sappi, Stora Enso, University of Aveiro, University of Twente, Valmet, VTT, WEPA and Zellstof Pöls. More information can be found on *https://ispt.eu/programs/deep-eutectic-solvents/*

Appendix A. Supplementary material

Supplementary data to this article can be found online at https://doi.org/10.1016/j.seppur.2022.122097.

References

[1] S. Chovau, D. Degrauwe, B. van der Bruggen, Critical analysis of techno-economic estimates for the production cost of lignocellulosic bio-ethanol, Renew. Sustain. Energy Rev. 26 (2013) 307–321, https://doi.org/10.1016/j.rser.2013.05.064.
[2] S. al Arni, Extraction and isolation methods for lignin separation from sugarcane bagasse: A review, Ind Crops Prod. 115 (2018) 330–339, https://doi.org/10.1016/j.indcrop.2018.02.012.
[3] J.N. Putro, F.E. Soetaredjo, S.-Y. Lin, Y.-H. Ju, S. Ismadji, Pretreatment and conversion of lignocellulose biomass into valuable chemicals, RSC Adv. 6 (2016) 46834–46852, https://doi.org/10.1039/C6RA09851G.
[4] A.D. Pérez, J. Fiskari, B. Schuur, Delignification of Low-Energy Mechanical Pulp (Asplund Fibers) in a Deep Eutectic Solvent System of Choline Chloride and Lactic Acid, Front Chem. 9 (2021), 688291, https://doi.org/10.3389/fchem.2021.688291.
[5] A.K. Singh, M. Bilal, H.M.N. Iqbal, A.S. Meyer, A. Raj, Bioremediation of lignin derivatives and phenolics in wastewater with lignin modifying enzymes: Status, opportunities and challenges, Sci. Total Environ. 777 (2021), 145988, https://doi.org/10.1016/j.scitotenv.2021.145988.
[6] N.D. Luong, N.T.T. Binh, L.D. Duong, D.O. Kim, D.-S. Kim, S.H. Lee, B.J. Kim, Y. S. Lee, J.-D. Nam, An eco-friendly and efficient route of lignin extraction from black liquor and a lignin-based copolyester synthesis, Polym. Bull. 68 (2012) 879–890, https://doi.org/10.1007/s00289-011-0658-x.
[7] L. Dessbesell, M. Paleologou, M. Leitch, R. Pulkki, C. Xu, Global lignin supply overview and kraft lignin potential as an alternative for petroleum-based polymers, Renew. Sustain. Energy Rev. 123 (2020), 109768, https://doi.org/10.1016/j.rser.2020.109768.
[8] M.N. Cabrera, M.F. Arrosbide, P. Franzoni, N. Cassella, Integrated forest biorefineries: green liquor extraction in eucalyptus wood prior to kraft pulping, Biomass Convers Biorefin. 6 (2016) 465–474, https://doi.org/10.1007/s13399-016-0203-0.
[9] M. Wang, L.D. Duong, Y. Ma, Y. Sun, S.Y. Hong, Y.C. Kim, J. Suhr, J.-D. Nam, A strategy to synthesize graphene-incorporated lignin polymer composite materials with uniform graphene dispersion and covalently bonded interface engineering, Korea-Australia Rheology Journal. 29 (2017) 207–213, https://doi.org/10.1007/s13367-017-0021-3.
[10] D.S. Zijlstra, C.W. Lahive, C.A. Analbers, M.B. Figueirêdo, Z. Wang, C.S. Lancefield, P.J. Deuss, Mild organosolv lignin extraction with alcohols: the importance of benzylic alkoxylation, ACS Sustain Chem Eng. 8 (2020) 5119–5131, https://doi.org/10.1021/acssuschemeng.9b07222.
[11] C.L. Yiin, K.L. Yap, A.Z.E. Ku, B.L.F. Chin, S.S.M. Lock, K.W. Cheah, A.C.M. Loy, Y. H. Chan, Recent advances in green solvents for lignocellulosic biomass pretreatment: Potential of choline chloride (ChCl) based solvents, Bioresour. Technol. 333 (2021), 125195, https://doi.org/10.1016/j.biortech.2021.125195.
[12] R. Roy, M.S. Rahman, D.E. Raynie, Recent advances of greener pretreatment technologies of lignocellulose, Curr. Res. Green Sustain. Chem. 3 (2020), 100035, https://doi.org/10.1016/j.crgsc.2020.100035.
[13] H. Xu, J. Peng, Y. Kong, Y. Liu, Z. Su, B. Li, X. Song, S. Liu, W. Tian, Key process parameters for deep eutectic solvents pretreatment of lignocellulosic biomass materials: a review, Bioresour Technol. 310 (2020), 123416, https://doi.org/10.1016/j.biortech.2020.123416.
[14] S.K. Bhatia, S.S. Jagtap, A.A. Bedekar, R.K. Bhatia, A.K. Patel, D. Pant, J. Rajesh Banu, C.V. Rao, Y.-G. Kim, Y.-H. Yang, Recent developments in pretreatment technologies on lignocellulosic biomass: Effect of key parameters, technological improvements, and challenges, Bioresour Technol. 300 (2020) 122724.
[15] W. Wang, D.-J. Lee, Lignocellulosic biomass pretreatment by deep eutectic solvents on lignin extraction and saccharification enhancement: a review, Bioresour Technol. 339 (2021), 125587, https://doi.org/10.1016/j.biortech.2021.125587.
[16] C. Alvarez-Vasco, R. Ma, M. Quintero, M. Guo, S. Geleynse, K.K. Ramasamy, M. Wolcott, X. Zhang, Unique low-molecular-weight lignin with high purity extracted from wood by deep eutectic solvents (DES): a source of lignin for valorization, Green Chem. 18 (2016) 5133–5141, https://doi.org/10.1039/C6GC01007E.
[17] X.-J. Shen, J.-L. Wen, Q.-Q. Mei, X. Chen, D. Sun, T.-Q. Yuan, R.-C. Sun, Facile fractionation of lignocelluloses by biomass-derived deep eutectic solvent (DES) pretreatment for cellulose enzymatic hydrolysis and lignin valorization, Green Chem. 21 (2019) 275–283, https://doi.org/10.1039/C8GC03064B.
[18] J.L.K. Mamilla, U. Novak, M. Grilc, B. Likozar, Natural deep eutectic solvents (DES) for fractionation of waste lignocellulosic biomass and its cascade conversion to value-added bio-based chemicals, Biomass Bioenergy. 120 (2019) 417–425, https://doi.org/10.1016/j.biombioe.2018.12.002.
[19] Y.T. Tan, A.S.M. Chua, G.C. Ngoh, Deep eutectic solvent for lignocellulosic biomass fractionation and the subsequent conversion to bio-based products – a review, Bioresour Technol. 297 (2020), 122522, https://doi.org/10.1016/j.biortech.2019.122522.
[20] B. Schuur, T. Brouwer, D. Smink, L.M.J. Sprakel, Green solvents for sustainable separation processes, Curr. Opin. Green Sustain. Chem. 18 (2019) 57–65, https://doi.org/10.1016/j.cogsc.2018.12.009.
[21] A.M. da Costa Lopes, J.R.B. Gomes, J.A.P. Coutinho, A.J.D. Silvestre, Novel insights into biomass delignification with acidic deep eutectic solvents: a mechanistic study of β-O-4 ether bond cleavage and the role of the halide counterion in the catalytic performance, Green Chem. 22 (2020) 2474–2487, https://doi.org/10.1039/C9GC02569C.
[22] D. Smink, A. Juan, B. Schuur, S.R.A. Kersten, Understanding the role of choline chloride in deep eutectic solvents used for biomass delignification, Ind. Eng. Chem. Res. 58 (2019) 16348–16357, https://doi.org/10.1021/acs.iecr.9b03588.
[23] A. Holtz, D. Weidener, W. Leitner, H. Klose, P.M. Grande, A. Jupke, Process development for separation of lignin from OrganoCat lignocellulose fractionation using antisolvent precipitation, Sep. Purif. Technol. 236 (2020), 116295, https://doi.org/10.1016/j.seppur.2019.116295.
[24] D. Smink, S.R.A. Kersten, B. Schuur, Comparing multistage liquid–liquid extraction with cold water precipitation for improvement of lignin recovery from deep eutectic solvents, Sep. Purif. Technol. 252 (2020), 117395, https://doi.org/10.1016/j.seppur.2020.117395.
[25] D. Smink, S.R.A. Kersten, B. Schuur, Recovery of lignin from deep eutectic solvents by liquid-liquid extraction, Sep. Purif. Technol. 235 (2020), 116127, https://doi.org/10.1016/j.seppur.2019.116127.
[26] D. Smink, S.R.A. Kersten, B. Schuur, Process development for biomass delignification using deep eutectic solvents. Conceptual design supported by experiments, Chem. Eng. Res. Des. 164 (2020) 86–101, https://doi.org/10.1016/j.cherd.2020.09.018.
[27] K. Servaes, A. Varhimo, M. Dubreuil, M. Bulut, P. Vandezande, M. Siika-aho, J. Sirviö, K. Kruus, W. Porto-Carrero, B. Bongers, Purification and concentration of lignin from the spent liquor of the alkaline oxidation of woody biomass through membrane separation technology, Ind. Crops Prod. 106 (2017) 86–96, https://doi.org/10.1016/j.indcrop.2016.10.005.
[28] A.-S. Jönsson, A.-K. Nordin, O. Wallberg, Concentration and purification of lignin in hardwood kraft pulping liquor by ultrafiltration and nanofiltration, Chem. Eng. Res. Des. 86 (2008) 1271–1280, https://doi.org/10.1016/j.cherd.2008.06.003.
[29] A. Toledano, A. García, I. Mondragon, J. Labidi, Lignin separation and fractionation by ultrafiltration, Sep. Purif. Technol. 71 (2010) 38–43, https://doi.org/10.1016/j.seppur.2009.10.024.
[30] J. Fernández-Rodríguez, X. Erdocia, F. Hernández-Ramos, M.G. Alriols, J. Labidi, in: Separation of Functional Molecules in Food by Membrane Technology, Elsevier, 2019, pp. 229–265.
[31] V. Ippolitov, I. Anugwom, R. van Deun, M. Mänttäri, M. Kallioinen-Mänttäri, Cellulose membranes in the treatment of spent deep eutectic solvent used in the recovery of lignin from lignocellulosic biomass, Membranes (Basel) 12 (1) (2022) 86.
[32] R.F. Madsen, Design of sanitary and sterile UF- and diafiltration plants, Sep Purif Technol. 22–23 (2001) 79–87, https://doi.org/10.1016/S1383-5866(00)00144-1.
[33] F. Lipnizki, Chapter 7 - Membrane Processes for the Production of Bulk Fermentation Products, in: Z.F. Cui, H.S. Muralidhara (Eds.), Membrane Technology, Butterworth-Heinemann, Oxford, 2010: pp. 121–153. Doi: 10.1016/B978-1-85617-632-3.00007-0.
[34] M.R. Stoner, N. Fischer, L. Nixon, S. Buckel, M. Benke, F. Austin, T.W. Randolph, B. S. Kendrick, Protein-solute interactions affect the outcome of ultrafiltration/diafiltration operations, J. Pharm. Sci. 93 (2004) 2332–2342, https://doi.org/10.1002/jps.20145.
[35] M. Ramos-Andrés, C. Andrés-Iglesias, J. García-Serna, Production of molecular weight fractionated hemicelluloses hydrolyzates from spent coffee grounds combining hydrothermal extraction and a multistep ultrafiltration/diafiltration, Bioresour. Technol. 292 (2019), 121940, https://doi.org/10.1016/j.biortech.2019.121940.
[36] C. Gavazzi-April, S. Benoit, A. Doyen, M. Britten, Y. Pouliot, Preparation of milk protein concentrates by ultrafiltration and continuous diafiltration: effect of process design on overall efficiency, J. Dairy Sci. 101 (2018) 9670–9679, https://doi.org/10.3168/jds.2018-14430.
[37] C.A.E. Costa, P.C.R. Pinto, A.E. Rodrigues, Lignin fractionation from E. Globulus kraft liquor by ultrafiltration in a three stage membrane sequence, Sep. Purif. Technol. 192 (2018) 140–151, https://doi.org/10.1016/j.seppur.2017.09.066.
[38] N.S. Kevlich, M.L. Shofner, S. Nair, Membranes for Kraft black liquor concentration and chemical recovery: current progress, challenges, and opportunities, Sep. Sci. Technol. 52 (2017) 1070–1094, https://doi.org/10.1080/01496395.2017.1279180.
[39] F. Lipnizki, J. Thuvander, G. Rudolph, Chapter 13 - Membrane processes and applications for biorefineries, in: A. Figoli, Y. Li, A. Basile (Eds.), Current Trends

and Future Developments on (Bio-) Membranes, Elsevier, 2020: pp. 283–301. Doi: 10.1016/B978-0-12-816778-6.00013-8.
[40] I. Tanistra, M. Bodzek, Preparation of high-purity sulphate lignin from spent black liquor using ultrafiltration and diafiltration processes, Desalination 115 (1998) 111–120, https://doi.org/10.1016/S0011-9164(98)00030-7.
[41] J.S. Vrouwenvelder, J.A.M. van Paassen, L.P. Wessels, A.F. van Dam, S.M. Bakker, The membrane fouling simulator: a practical tool for fouling prediction and control, J. Memb. Sci. 281 (2006) 316–324, https://doi.org/10.1016/j.memsci.2006.03.046.
[42] K. Xiao, Y. Shen, X. Huang, An analytical model for membrane fouling evolution associated with gel layer growth during constant pressure stirred dead-end filtration, J. Memb. Sci. 427 (2013) 139–149, https://doi.org/10.1016/j.memsci.2012.09.049.
[43] J. Hermia, Blocking Filtration. Application to Non-Newtonian Fluids, in: A. Rushton (Ed.), Mathematical Models and Design Methods in Solid-Liquid Separation, Springer Netherlands, Dordrecht, 1985: pp. 83–89. Doi: 10.1007/978-94-009-5091-7_5.
[44] T. Zhu, Z. Zhou, F. Qu, B. Liu, B. van der Bruggen, Separation performance of ultrafiltration during the treatment of algae-laden water in the presence of an anionic surfactant, Sep. Purif. Technol. 281 (2022), 119894, https://doi.org/10.1016/j.seppur.2021.119894.
[45] A.Y. Kirschner, Y.-H. Cheng, D.R. Paul, R.W. Field, B.D. Freeman, Fouling mechanisms in constant flux crossflow ultrafiltration, J. Memb. Sci. 574 (2019) 65–75, https://doi.org/10.1016/j.memsci.2018.12.001.
[46] K.L. Chen, L. Song, S.L. Ong, W.J. Ng, The development of membrane fouling in full-scale RO processes, J. Memb. Sci. 232 (2004) 63–72, https://doi.org/10.1016/j.memsci.2003.11.028.
[47] W. Li, X. Su, A. Palazzolo, S. Ahmed, Numerical modeling of concentration polarization and inorganic fouling growth in the pressure-driven membrane filtration process, J. Memb. Sci. 569 (2019) 71–82, https://doi.org/10.1016/j.memsci.2018.10.007.
[48] J. Domínguez-Robles, T. Tamminen, T. Liitiä, M.S. Peresin, A. Rodríguez, A.-S. Jääskeläinen, Aqueous acetone fractionation of kraft, organosolv and soda lignins, Int. J. Biol. Macromol. 106 (2018) 979–987, https://doi.org/10.1016/j.ijbiomac.2017.08.102.
[49] Alfa Laval, Standard sizes Membrane type Sheets 20 x 20 cm Alfa Laval module M10 Alfa Laval module M20 Alfa Laval module M37 Alfa Laval module M38, n.d. www.alfalaval.com.
[50] H. Choi, K. Zhang, D.D. Dionysiou, D.B. Oerther, G.A. Sorial, Effect of permeate flux and tangential flow on membrane fouling for wastewater treatment, Sep. Purif. Technol. 45 (2005) 68–78, https://doi.org/10.1016/j.seppur.2005.02.010.
[51] A.-S. Jönsson, Influence of shear rate on the flux during ultrafiltration of colloidal substances, J. Membr. Sci. 79 (1993) 93–99, https://doi.org/10.1016/0376-7388(93)85020-W.
[52] L. Wang, L. Song, Flux decline in crossflow microfiltration and ultrafiltration: experimental verification of fouling dynamics, J. Memb. Sci. 160 (1999) 41–50, https://doi.org/10.1016/S0376-7388(99)00075-7.
[53] L. Song, Flux decline in crossflow microfiltration and ultrafiltration: mechanisms and modeling of membrane fouling, J. Memb. Sci. 139 (1998) 183–200, https://doi.org/10.1016/S0376-7388(97)00263-9.
[54] D.E. Wiley, C.J.D. Fell, A.G. Fane, Optimisation of membrane module design for brackish water desalination, Desalination 52 (1985) 249–265, https://doi.org/10.1016/0011-9164(85)80036-9.
[55] S. Lee, Performance comparison of spiral-wound and plate-and-frame forward osmosis membrane module, Membranes (Basel). 10 (2020) 318, https://doi.org/10.3390/membranes10110318.
[56] G. Schock, A. Miquel, Mass transfer and pressure loss in spiral wound modules, Desalination 64 (1987) 339–352, https://doi.org/10.1016/0011-9164(87)90107-X.
[57] A.I. Cavaco Morão, A.M. Brites Alves, V. Geraldes, Concentration polarization in a reverse osmosis/nanofiltration plate-and-frame membrane module, J. Memb. Sci. 325 (2008) 580–591, https://doi.org/10.1016/j.memsci.2008.08.030.
[58] Y. Roy, M.H. Sharqawy, J.H. Lienhard, Modeling of flat-sheet and spiral-wound nanofiltration configurations and its application in seawater nanofiltration, J. Memb. Sci. 493 (2015) 360–372, https://doi.org/10.1016/j.memsci.2015.06.030.
[59] A. Nishimoto, S. Yoshikawa, S. Ookawara, A model for transport phenomena in a cross-flow ultrafiltration module with microchannels, Membranes (Basel). 1 (2011) 13–24, https://doi.org/10.3390/membranes1010013.